Heavy neodymium isotopes in the interacting boson (IBA-2) model

A. Giannatiempo
Dipartimento di Fisica e Astronomia, Università di Firenze, I-50019 Sesto Fiorentino (Firenze), Italy and Istituto Nazionale di Fisica Nucleare, Sezione di Firenze, I-50019 Sesto Fiorentino (Firenze), Italy
(Received 24 February 2011; revised manuscript received 29 June 2011; published 15 August 2011)

The $N > 82$ even neodymium isotopes were studied in the framework of the IBA-2 model. The analysis was performed by using a very schematic Hamiltonian, particularly suited to investigate the U(5) $\rightarrow$ SU(3) transition. The evolution of the excitation energy patterns and of the spectroscopic properties along the isotopic chain can be correctly reproduced when the role played by states of mixed symmetry character is also taken into account.

DOI: 10.1103/PhysRevC.84.024308 PACS number(s): 21.10.Re, 21.60.Fw, 27.60.+j

I. INTRODUCTION

In recent years the study of nuclear shape/phase transitions that occur when the number of nucleons changes has been the subject of many experimental and theoretical works [1–28]. Models based on algebraic Hamiltonians, which are well suited to investigate phase transitions, were extensively applied to nuclei belonging to different mass regions. In these models the nuclear shapes among which the transition takes place are associated to dynamic symmetries, from which analytic solutions for the relevant observables can be obtained. In the framework of the interacting boson approximation (IBA) model [29], the analyses are usually carried out in the IBA-1 version, in which no distinction is made between proton pairs and neutron pairs and three dynamic symmetries exist, U(5), O(6), and SU(3), associated with a spherical, γ-unstable, and axially deformed shape, respectively.

Recently, the phase structure of a two-fluid bosonic system was investigated [13–15,18,19], considering the IBA-2 version [29–32] of the model. In this model proton pairs and neutron pairs are treated as distinct constituents and, in addition to the three symmetries of the IBA-1 version, a fourth symmetry exists, where proton and neutron fluids have different deformation. Because each bosonic fluid can exist in a different phase, their interplay gives rise to a more involved phase diagram which shows qualitatively new features.

The study of the transition region in isotopic chains undergoing a sharp change in structure has received particular attention since Iachello [33,34] introduced the E(5) and X(5) analytic solutions (under some simplifying approximations) of the collective Bohr Hamiltonian [35], corresponding to the critical points of a spherical to γ-unstable transition and a spherical to axially symmetric rotor transition, respectively. A transition region extensively investigated is that around $A \approx 150$, where ^{150}Nd [4] and ^{152}Sm [1] were first identified as nuclei displaying an X(5) character.

The sharp change from a spherical to an axially deformed structure of the heavier neodymium isotopes can be inferred from Fig. 1. Here, the excitation energy ratio of the 4_1^+ state to the 2_1^+ state, which is one of the usual benchmarks used in assessing collectivity, is reported as a function of the neutron number, N, and atomic mass, A, together with the values predicted by the U(5) and SU(3) symmetries.

In the present work even $^{144-156}$Nd isotopes are investigated in the framework of the IBA-2 model. This study is part of a more general one concerning the whole isotopic chain, $^{128-156}$Nd, with the obvious exception of the $N = 82$ ^{142}Nd isotope. A previous IBA-2 analysis of the excitation energies of low-lying levels up to $J = 8$ in $^{146-152}$Nd isotopes was performed a long time ago by Scholten [36], who obtained a good agreement with the experimental data.

The present analysis was performed by using a schematic Hamiltonian, suitable to study the U(5) to SU(3) transition. In the attempt at describing as completely as possible the evolution of the collective structure along the isotopic chain, states of fully symmetric (FS) as well as of mixed-symmetry (MS) character in the proton and neutron degrees of freedom were considered. The lowest-lying MS state has $J^\pi = 2^+$ in nuclei close to the U(5) limit and $J^\pi = 1^+$ in nuclei close to the SU(3) limit. Additional information on structural changes for increasing A could thus be provided by the identification of these states. Calculations of excitation energies, quadrupole moments, $E2$ and $M1$ strengths, $E2/M1$ mixing ratios, and intensity ratios were carried out. The analysis of the g factors in $^{144-150}$Nd, which allows one to extend the comparison on the spectroscopic properties of the heavy neodymium isotopes, is presented in a separate paper.

In Sec. II, the IBA-2 Hamiltonian used and the criteria adopted for the determination of the model parameters are described. The comparison of the numerical results with the experimental data and the discussion about the structure of the isotopes is reported in Sec. III. Finally, in Sec. IV the main conclusions of this study are drawn.

II. THE IBA-2 HAMILTONIAN

The schematic Hamiltonian adopted in the present study retains the main ingredients of the most general ones and it has been used in this form since the earlier IBA-2 analyses (see, e.g., Refs. [37–39]). It is similar to that usually adopted in the IBA-1 studies of the U(5) $\rightarrow$ SU(3) transition [40,41], which only contains the d-boson number operator, $\hat{n}_d$, and the quadrupole-quadrupole operator, $\hat{Q}^{(\chi)} \cdot \hat{Q}^{(\chi)}$, with $Q^{(\chi)} = (s^\dagger \tilde{d} + d^\dagger \tilde{s}) + \chi(d^\dagger \tilde{d})$. Here, the parameter χ is kept to the value $-\sqrt{7}/2$, which characterizes the SU(3) symmetry. The transition is therefore controlled by a single parameter, which essentially determines the relative strength of the spherical-driving $\hat{n}_d$ term and the deformation-driving quadrupole interaction.

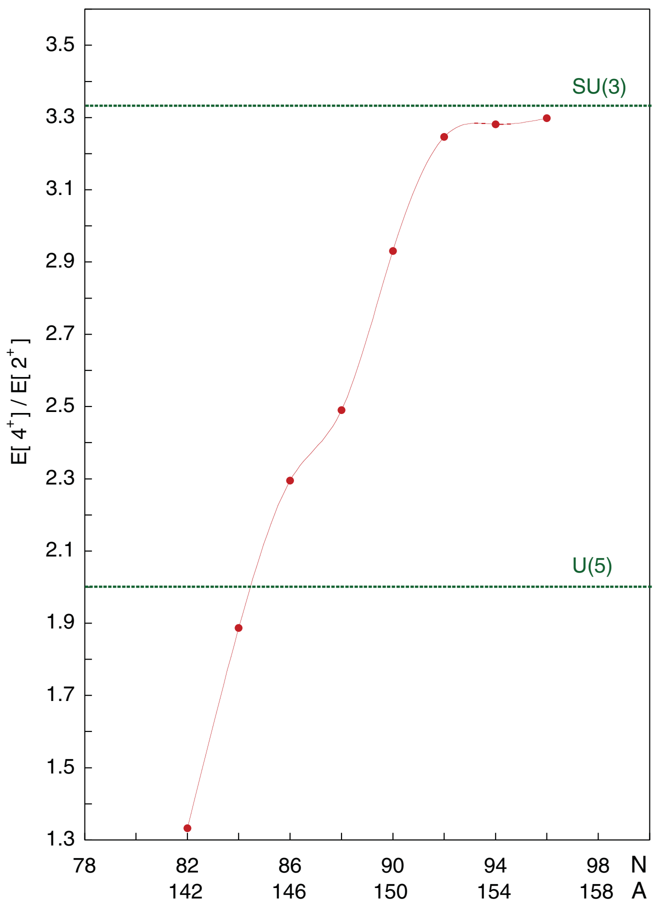

FIG. 1. (Color online) Evolution of the energy ratio of the 4_1^+ state to the 2_1^+ state as a function of the neutron number and atomic mass number in even neodymium isotopes with $N \geqslant 82$. The horizontal lines show the values predicted by the U(5) and SU(3) limits of the IBA model.

Accordingly, the adopted IBA-2 Hamiltonian,

$$H = \varepsilon_\pi\, \hat{n}_{d_\pi} + \varepsilon_\nu\, \hat{n}_{d_\nu} + \kappa\, \hat{Q}_\pi^{(\chi_\pi)} \cdot \hat{Q}_\nu^{(\chi_\nu)} + \hat{M}_{\pi\nu}$$

(with $\chi_\pi = \chi_\nu = -\sqrt{7}/2$) contains only the physically dominant interactions, i.e., the like-nucleon pairing $\hat{n}_{d_\rho}$ ($\rho = \pi, \nu$) and the π-, ν-boson quadrupole interaction. The usual practice of putting $\varepsilon_\pi = \varepsilon_\nu = \varepsilon$ was followed to keep to a minimum the numbers of free parameters.

In the framework of the IBA-2 model, the Majorana term ($\hat{M}_{\pi\nu}$ operator) is added to properly account for states not fully symmetric in the proton and neutron degrees of freedom. In the present work the generalized Majorana operator [42] was used:

$$\hat{M}_{\pi\nu} = \frac{1}{2}\xi_2[s_\nu^\dagger d_\pi^\dagger - s_\pi^\dagger d_\nu^\dagger]^{(2)} \cdot [\tilde{s}_\nu \tilde{d}_\pi - \tilde{s}_\pi \tilde{d}_\nu]^{(2)}$$
$$- \xi_1[d_\nu^\dagger d_\pi^\dagger]^{(1)} \cdot [\tilde{d}_\nu \tilde{d}_\pi]^{(1)} - \xi_3[d_\nu^\dagger d_\pi^\dagger]^{(3)} \cdot [\tilde{d}_\nu \tilde{d}_\pi]^{(3)}.$$

The parameters ξ_1, ξ_2, ξ_3 are allowed to assume independent values so that it is possible to take into account the different effects of each of them on the relevant states (see, e.g., Ref. [43]). The symmetry character of a state is related to the value of the F-spin quantum number. Fully symmetric states have $F = F_{\max} = N_B/2$ (where $N_B = N_\pi + N_\nu$ is the total number of bosons), whereas MS states have $F = F_{\max} - 1, F_{\max} - 2, \ldots$, etc. The degree of symmetry of a state that contains both FS and MS components is related to its F-spin components.

The Hamiltonian was diagonalized by using the NPBOS code [44] which, for any given state, calculates the squared amplitude of its F-spin components.

In the following the squared amplitude of the $F = F_{\max}$ component is indicated by α^2. The $E2$ and $M1$ operators are given by

$$\hat{T}(E2) \equiv e_\nu \hat{T}_\nu(E2) + e_\pi \hat{T}_\pi(E2) \;=\; e_\nu \hat{Q}_\nu^{(\chi_\nu)} + e_\pi \hat{Q}_\pi^{(\chi_\pi)},$$
$$\hat{T}(M1) \equiv g_\nu \hat{T}_\nu(M1) + g_\pi \hat{T}_\pi(M1) = \sqrt{\frac{3}{4\pi}}(g_\nu \hat{L}_\nu + g_\pi \hat{L}_\pi),$$

where e_ρ and g_ρ are the effective quadrupole charges and gyromagnetic ratios, respectively. The values of χ_ρ are the same as in the Hamiltonian (consistent-Q formalism [45,46]).

In the analysis one has to consider somehow the possible effects induced by the subshell closure at $Z = 64$ on Nd isotopes having $N \leqslant 90$. The abrupt increase in collectivity observed in the region near $N = 90$ is ascribed (see, e.g., Ref. [47]) to the obliteration of the gap at $Z = 64$ caused by the isospin $T = 0$ component of the p-n interaction (which involves chiefly the spin-orbit partners) when neutrons begin to fill the $h_{9/2}$ orbit, thereby inducing a reduction of the effective single-particle energy of the $h_{11/2}$ proton orbit.

To take into account such an effect, one can count the proton-boson number N_π in the *normal* way, i.e., with respect to the closed shell at $Z = 50$, and allow the proton effective charges, e_π, and gyromagnetic ratios, g_π, to change when N increases from 84 to 88. Alternatively, one can consider an *effective* N_π^{eff} value for each $^{144-148}$Nd isotope [$N = 84$–88] and keep e_π and g_π at fixed values (see, e.g., Ref. [48]).

In both cases the neutron-boson number, N_ν, is counted with respect to the $N = 82$ closed shell, so that, in $^{144-1156}$Nd isotopes, its value ranges from 1 to 7. In the present analysis, where the first approach was followed, one has $N_\pi = 5$. The parameters e_ν and g_ν were kept fixed for all isotopes, and the parameters e_π and g_π were kept fixed for $^{150-156}$Nd but were allowed to vary in $^{144-148}$Nd.

A study performed in the framework of the IBA-2 model implies, of course, neglecting noncollective degrees of freedom. To this aim, for each Nd isotope only the yrast states having an excitation energy up to the back-bending region were considered, with the only exception being the 4_1^+ state in ^{144}Nd. The criteria on which the selection of the non-yrast states of collective nature was based are discussed separately for the different isotopes (see Sec. III A).

The Hamiltonian parameters, ε and κ, were determined so as to reproduce as closely as possible the excitation energies of the ground-state (g.s.) band in each isotope. As to the Majorana parameters, they do not influence at all FS states and affect differently states of MS character. This is particularly clear when referring to the U(5) limit of the model, where the excitation energies of MS states belonging

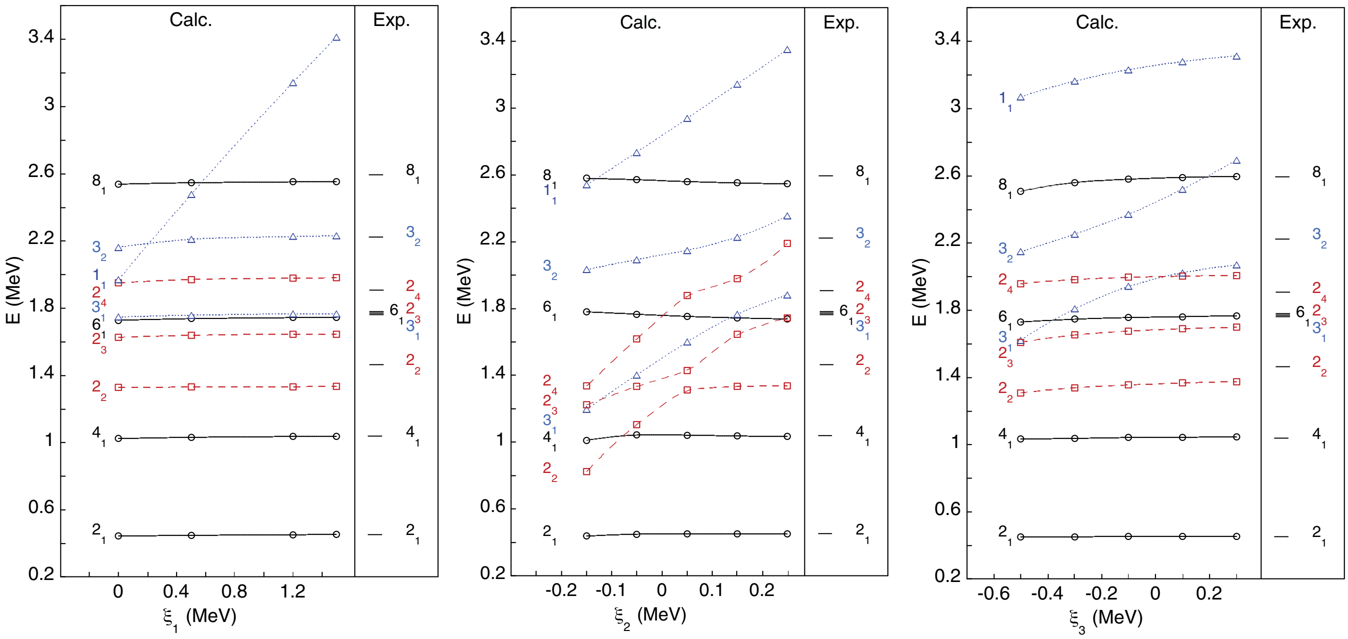

FIG. 2. (Color online) Excitation energies of ^{146}Nd, calculated as a function of (left) ξ_1 (for $\xi_2 = 0.15$ and $\xi_3 = -0.35$ MeV), (center) ξ_2 (for $\xi_1 = 1.2$ and $\xi_3 = -0.35$ MeV), (right) ξ_3 (for $\xi_1 = 1.2$ and $\xi_2 = 0.15$ MeV), are compared to the experimental data. The calculated values for the states of ground-state (g.s.) bands are connected by a solid line, for the 2_2^+, 2_3^+, and 2_4^+ states by a dashed line, and for the 1_1^+, 3_1^+, and 3_2^+ states by a dotted line.

to different irreducible representations are given in analytical form [49–51] as a function of ξ_1, ξ_2, and ξ_3. States having $F = F_{\max} - 1$ can be arranged in three groups (see, e.g., Fig. 1 of Ref. [50]) and their excitation energies depend on

(i) ξ_2 (all groups),
(ii) ξ_3 (states of the groups having as the lowest level the 1^+ or 3^+ state), and
(iii) ξ_1 (states of the group having as the lowest level the 1^+ state).

An example of the procedure followed to deduce the values of the Majorana parameters is given in Fig. 2. Here, the excitation energies of the relevant states of ^{146}Nd as ξ_1 (left), ξ_2 (middle), or ξ_3 (right) are varied, while keeping the other two parameters fixed to their finally adopted values, are shown. As expected (small value of the ratio κ/ε), the influence of the different Majorana parameters on excitation energies of states containing large MS components is quite close to that mentioned earlier for the U(5) limit. One can notice the sizable modification of the excitation energy pattern, which ensues from the presence of MS states at low energy. The final choice of the ξ_2 and ξ_3 values was performed through a lengthy procedure where these parameters were varied in small steps along a restricted range of values, checking, at each step, how the calculated electromagnetic (e.m.) properties of the relevant states compared to the experimental data.

As to ξ_1, it is seen that it substantially affects only the excitation energy of the 1^+ state. This fact has been taken into account in the attempt at identifying the lowest 1^+ MS state in $^{144-150}$Nd, where several $J = 1$ states are known. To avoid an identification based only on excitation energies, which can always be reproduced through a proper choice of ξ_1, transition strengths and branching ratios [52,53] were also considered. The possible candidates were required to display a smooth trend of the excitation energies and an increasing strength of the transition to the ground state for increasing A. In particular, the $B(M1; 1_1^+ \rightarrow 0_1^+)$ strength was required to increase as the deformation increases, because its value is zero in the U(5) limit and takes a finite value in the SU(3) limit. However, several states have no definite parity assignment, as is the case for all the $J = 1$ states in ^{148}Nd and for the lowest $J = 1$ state in ^{150}Nd. Furthermore, it was not possible to find states having the required aforementioned characteristics. For example, the $B(M1; 1^+ \rightarrow 0_1^+)$ strengths of the states with definite assignment $J^\pi = 1^+$ in ^{146}Nd are larger than almost all those measured in ^{148}Nd. Because of the difficulty of a clear identification of the 1_1^+ MS state, in $^{144-150}$Nd the ξ_1 value was arbitrarily kept at 1.2 MeV, so as to push the lowest predicted 1^+ state to high energy, without performing any fit to the experimental data.

In $^{152-156}$Nd it was not possible to determine the Majorana parameters because of the lack of any experimental information providing some hint for their choice. Their values were arbitrarily kept at 0.5 MeV, having checked that changes in the range 0–1.5 MeV do not affect the predicted excitation energies and decay properties of the states considered in the analysis.

The values obtained for the parameters ε, κ, ξ_2, and ξ_3, as a function of the mass number, are shown in Fig. 3. The trend of ξ_2, and ξ_3 in $^{144-150}$Nd isotopes, which are at the beginning of the neutron major shell $N = 82$–126, is similar to that found in Ru [54] and in Pd [50] isotopic chains at the beginning of

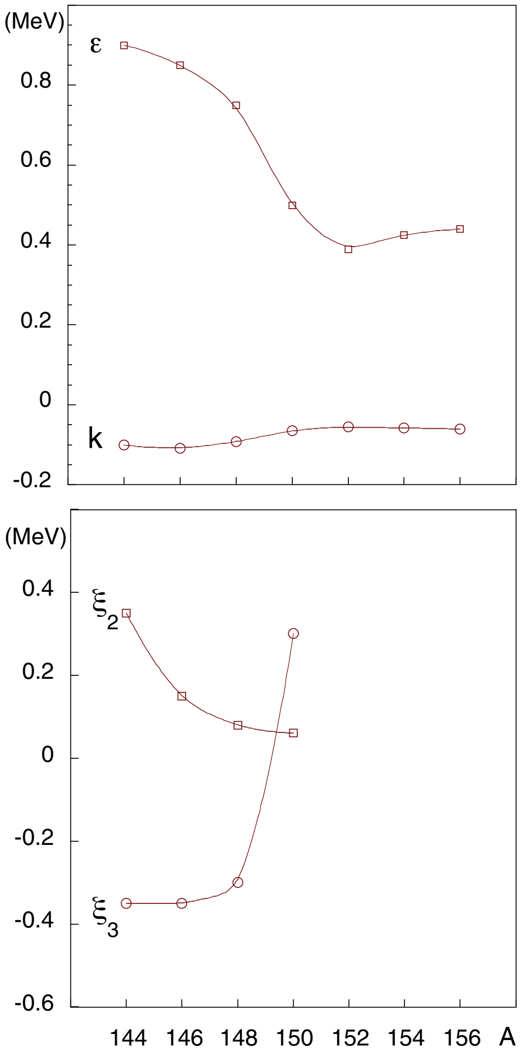

FIG. 3. (Color online) Values of the Hamiltonian parameters varied in the analysis as a function of the atomic number A.

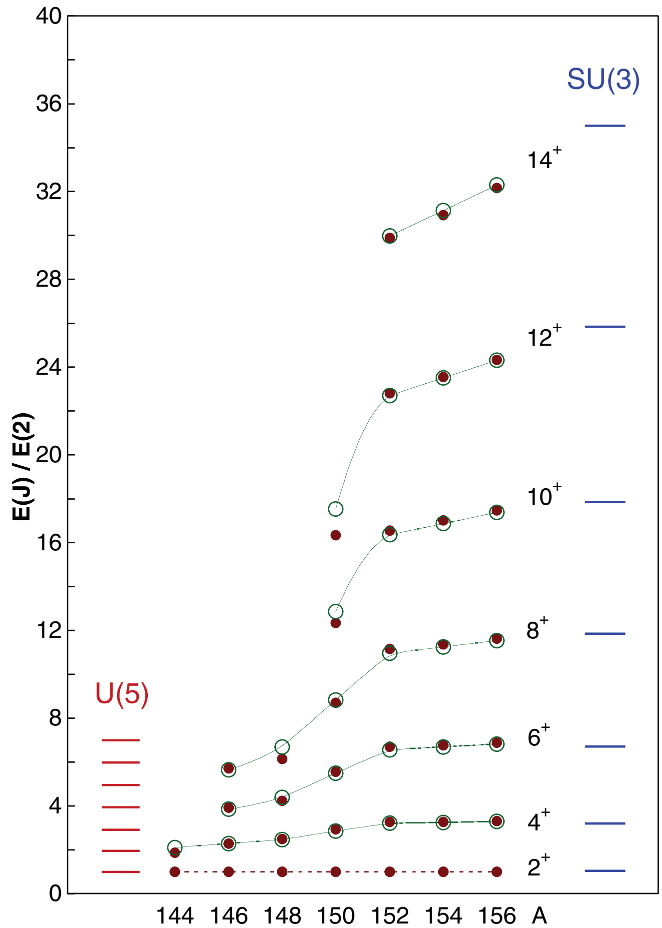

FIG. 4. (Color online) Comparison of experimental (solid circles) and calculated (open circles) *normalized* energies of the relevant states of the g.s. bands in $^{144-156}$Nd isotopes, including the relative energies predicted by the U(5) (left) and SU(3) (right) limits of the IBA-2 model for the states with J up to 14.

the major shell $N = 50$–82. Indeed, the value of ξ_2 is high and positive near the neutron close shell and decreases going toward the neutron midshell, whereas ξ_3 has an opposite trend. These parameters display, therefore, the same neutron-number dependence at the beginning of a major shell in different mass regions.

As to the parameters appearing in the e.m. operators, the effective quadrupole charges were extracted through a fit to the *experimental* absolute values of $\langle J_f \| \hat{T}(E2) \| J_i \rangle$, obtained from the data available on quadrupole moments and $B(E2)$ reduced transition probabilities in $^{150-152}$Nd. The deduced values are $e_\pi = 0.18$ e b and $e_\nu = 0.097$ e b.

The value of e_ν was kept fixed all along the isotopic chain and that of e_π was used in the analysis of $^{150-156}$Nd, whereas for the lighter isotopes it was determined, for each isotope, from the experimental $B(E2)$ values of the g.s. band. The values extracted for e_π are 0.105, 0.110, and 0.140 e b in ^{144}Nd, ^{146}Nd, and ^{148}Nd, respectively.

For the gyromagnetic ratios, the values deduced by Wolf and Casten [48] from the analysis of nuclei in the $A \approx 150$ region were partially used. Those authors took into account the nuclei with $N \geqslant 90$, for which it was possible to assume that

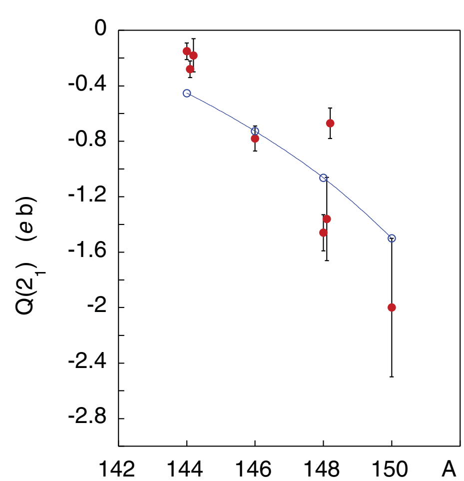

FIG. 5. (Color online) Experimental results of quadrupole moments of the 2_1^+ state in $N > 82$ neodymium isotopes are compared to the calculated ones (open circles).

the values of N_π and N_ν were the *normal* ones, and extracted, at the same time, the effective boson charges ($e_\pi = 0.169$, $e_\nu = 0.095\,e$ b) and gyromagnetic ratios ($g_\pi = 0.63$, $g_\nu = 0.05\mu_N$). The values of all e.m. parameters were then kept fixed to extract the *effective* $N_\pi^{\rm eff}$ values for the $N = 84$–88 nuclei.

Because of the different approach followed in the present work, it was possible to adopt $g_\nu = 0.05\mu_N$ in the analysis of all the Nd isotopes and $g_\pi = 0.63\mu_N$ in that of $^{150-156}$Nd; however, it was necessary to evaluate separately the value of g_π for each $^{144-148}$Nd isotope. To this aim, a linear relation between g_π and e_π was assumed, on the basis of the relationship connecting dipole moments and atomic number Z in collective models ($\mu \propto Z/A$) [35]. The value of g_π for different A (< 150) was obtained by simply scaling from the value $e_\pi = 0.18\,e$ b and $g_\pi = 0.63\mu_N$ according to the relation

$$g_\pi(A) = [e_\pi(A)/0.18]0.63\mu_N.$$

In this way, g_π turns out to be $0.367\mu_N$ in ^{144}Nd, $0.385\mu_N$ in ^{146}Nd, and $0.49\mu_N$ in ^{148}Nd. It is worth mentioning that the values extracted in the present work for e_π and e_ν from the analysis of $^{150-156}$Nd are very close to those reported by Wolf and Casten [48].

III. RESULTS AND DISCUSSION

In this section, after some general comments concerning the isotopic chain ($N > 82$), the results obtained for each isotope are discussed in detail. The experimental data are from Ref. [53], except for those quoted separately.

In Fig. 4 are shown the states of the g.s. bands in $^{144-156}$Nd considered in the analysis. It is seen that their number reduces dramatically when the neutron number approaches the $N = 82$ shell closure. The experimental excitation energies, normalized to that of the 2_1^+ state, are compared to the calculated ones and to the predictions of the U(5) and SU(3) limits. All the states reported in the figure turn out to have $\alpha^2 > 0.96$, so their predicted energies are not actually affected by the Majorana parameters. Since χ_π and χ_ν are fixed, the calculated energies are determined only by the parameters ε and κ. On the average, they match the experimental ones to better than 0.4%, so it turns out that the U(5) → SU(3) transition along the isotopic chain is well reproduced by the calculations as far as the excitation energies of the g.s. band are concerned.

In Fig. 5 the available experimental data [55] on the quadrupole moments of the 2_1^+ state, $Q(2_1^+)$, in the isotopic chain are compared to the calculated ones. The sign of the quadrupole moments and the increase of the absolute values for increasing A are correctly reproduced. This provides a first indication about the validity of the choice performed for χ_π, χ_ν, and the effective charges.

A. ^{144,146,148}Nd

The results concerning these isotopes are discussed simultaneously because of their common features. They are characterized by a structure close to, or not too far from, the U(5) symmetry and by the fact that several transitions connecting low-lying states have large $M1$ components.

TABLE I. The available experimental $B(M1)$ reduced transition strengths in Nd isotopes compared to the calculated ones. The values are given in μ_N^2 units.

A	$J_i^\pi \to J_f^\pi$	E_γ (MeV)	$B(M1)_{\rm expt}$	$B(M1)_{\rm calc}$
144	$2_2^+ \to 2_1^+$	0.697	0.056(7)	0.001
144	$2_3^+ \to 2_1^+$	1.376	0.12(5)	0.02
144	$2_4^+ \to 2_1^+$	1.672	0.18(7)	0.01
144	$3_1^+ \to 2_1^+$	1.482	0.036^{+53}_{-25}	0.001
144	$3_1^+ \to 4_1^+$	0.864	0.38(28)	0.001
148	$2_2^+ \to 2_1^+$	0.869	0.0005^{+18}_{-5}	0.0001

As is well known, $M1$ transitions are forbidden between $F = F_{\rm max}$ states, whereas they can connect states having $\Delta F = \pm 1$ [39,56]. Unusually large $M1$ transitions and/or small $E2/M1$ mixing ratios ($|\delta| \leqslant\approx 0.3$) are therefore considered important signatures for the identification of MS states [39,57]. However, enhanced probabilities for $M1$ transitions could be due to two-quasiparticle configurations in the initial and final states. In particular, $(2f_{7/2})_\nu^n$ configurations may play an important role in determining the structure of the states even at low energy, as pointed out by several authors (see, e.g., Ref. [58]).

One of the aims of the present work was therefore to test to what extent the calculations could reproduce the experimental data once states of MS character were also taken into account, still with the awareness of the possible interplay of collective and single-particle degrees of freedom. Indeed, the importance of single-particle structural influence on low-lying levels of these isotopes is already apparent when considering the 4_1^+ state in ^{144}Nd: the energy ratio $R_{4/2}$ (1.9) is smaller than the lower limit 2, commonly accepted for collective states, and the $B(E2;4_1^+ \to 2_1^+)/B(E2;2_1^+ \to 0_1^+)$ ratio (0.98 ± 3) [59] is considerably smaller than the value of 1.6 predicted by the U(5) limit for a six-boson nucleus.

The levels considered in the analysis of these isotopes are those reported in Fig. 4, the 0_2^+ state in ^{148}Nd, the 2_2^+, 2_3^+, and 2_4^+ states, and the 3_1^+ and 3_2^+ state in $^{144-148}$Nd. This restricted choice was due to the following reasons:

(i) The 0_2^+, 2085-keV state in ^{144}Nd and the 0_2^+, 1603- keV and 0_3^+, 1697-keV states in ^{146}Nd have energies that are nearly three times that of the 2_1^+ state and decay through a γ transition only to the 2_1^+ state. Therefore, they do not match the properties of the lower 0^+ states in nuclei having a structure close to the U(5) limit either for the 0_2^+ state, because of the excitation energies, or for the 0_3^+ state, because of the γ decay.

(ii) In ^{146}Nd the existence of a 0^+ state at 915 keV (about twice the energy of the 2_1^+ state), reported as doubtful in Ref. [53], and of a 2^+ state at 1303 keV was excluded by Demidov *et al.* [60], who did not observe these states in the inelastic scattering of fast neutrons.

(iii) In ^{148}Nd, two bands, built on the 0_2^+ and the 2_3^+ states, respectively, are reported in Ref. [53]. In both cases no in-band γ transitions were observed, so the existence of such bands seems unlikely.

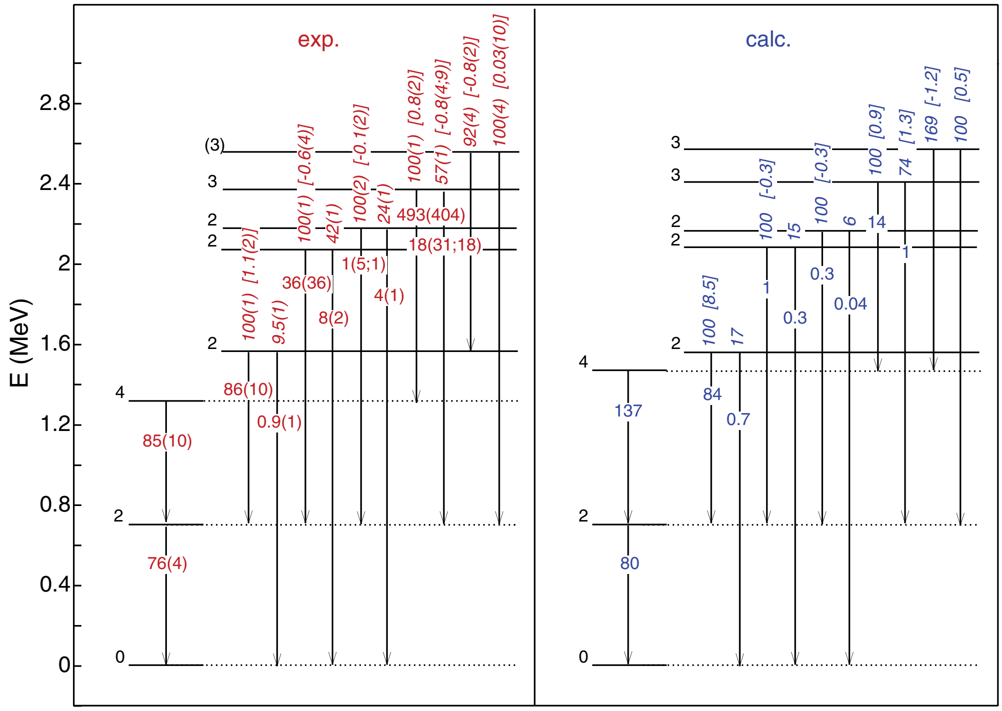

FIG. 6. (Color online) Comparison of experimental and predicted excitation energies, $B(E2)$ transition strengths (reported on the transition arrows in 10^{-3} e^2 b^2 units), and (vertical writing) relative intensities and mixing ratios (in square brackets) for ^{144}Nd. Asymmetric errors are shown as two values, the first one corresponding to the positive value.

(iv) In $^{144-148}$Nd, apart from the states of the g.s. band, no state having $J \geqslant 4$ displays properties compatible with a collective structure.

The low-lying 2^+states are of particular interest for the present analysis because, in nuclei close to the U(5) limit, the lowest MS state is predicted to have $J^\pi = 2^+$. It is

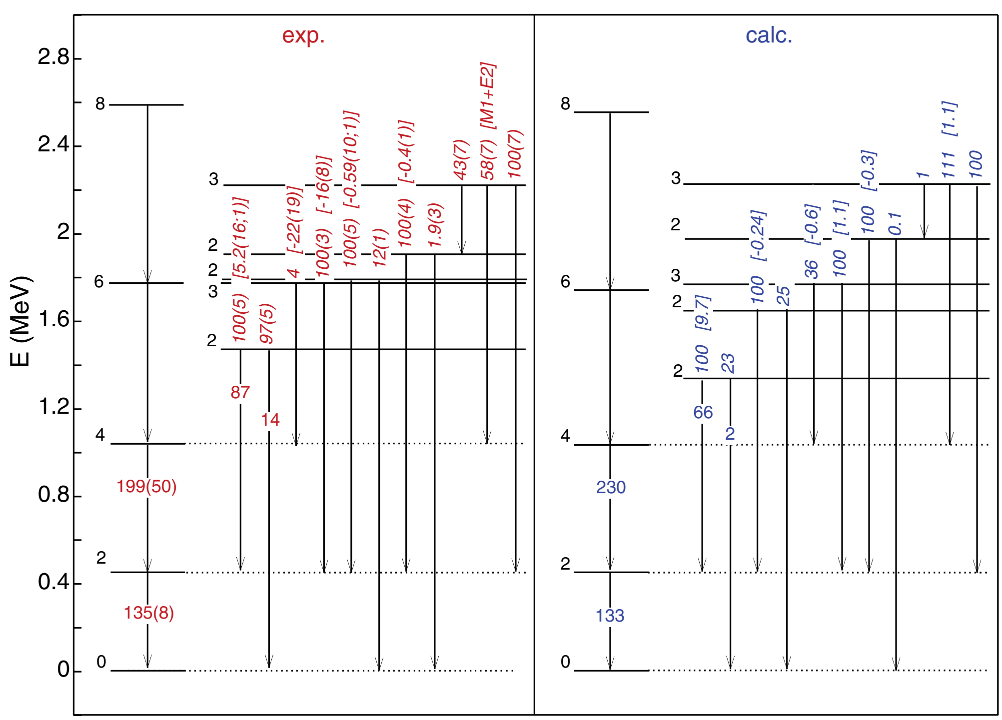

FIG. 7. (Color online) As in Fig. 6, but for ^{146}Nd. The $B(E2; 2_2^+ \rightarrow 0_1^+)$ and $B(E2; 2_2^+ \rightarrow 2_1^+)$ values are given without errors because they were deduced from the half-life (≈0.3 ps) of the 2_2^+ level reported in Ref. [53].

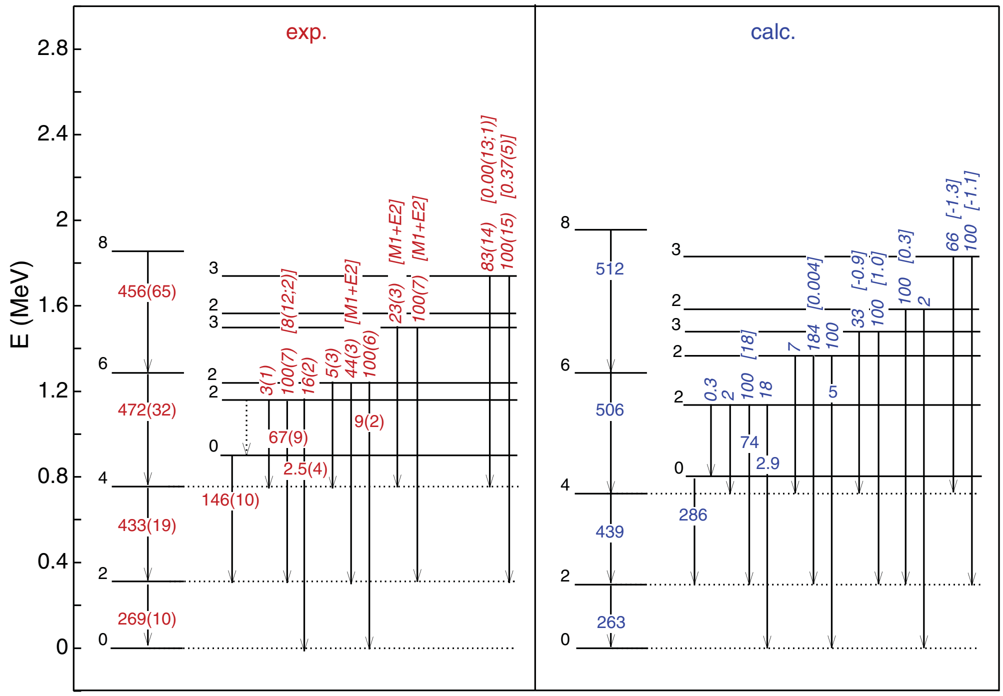

FIG. 8. (Color online) As in Fig. 6, but for ^{148}Nd. The γ decay of the 2_4^+ state at 1577 keV is unknown.

characterized by a preferential decay to the 2_1^+ state through an $M1$ transition [29].

As to the 3^+ states, in the IBA-2 studies of the Kr ($Z = 36$) [61], Ru ($Z = 44$) [50,54], and Pd ($Z = 46$) [[50] isotopic chains, it turned out that the possibility of reproducing correctly the properties of the 3_1^+ state relied, in most cases, on important MS components present in its wave function.

The results of the present study on excitation energies, $B(E2)$ values, relative intensities, and $\delta(E2/M1)$ mixing ratios of the transitions deexciting the relevant states are shown in Figs. 6, 7, and 8, whereas those on the available $B(M1)$ reduced transition strengths are given in Table I. For the sign of the $\delta[E(2)/M(1)]$ mixing ratio, Krane and Steffen's convention [62] was adopted. This implies changing the sign of the experimental mixing ratios in ^{144}Nd with respect to those reported in Ref. [53].

The experimental value shown in Fig. 6 for the $B(E2; 2_1^+ \rightarrow 0_1^+)$ reduced strength in ^{144}Nd is from Ref. [63]. The choice of this value, with respect to that reported in Ref. [53], is due to its better agreement with the $B(E2; 4_1^+ \rightarrow 2_1^+)/B(E2; 2_1^+ \rightarrow 0_1^+)$ ratio, which was recently measured [59].

By looking at Figs. 6, 7, and 8, it appears that the calculations are able to reproduce the evolution of the g.s. band from ^{144}Nd to ^{148}Nd, i.e., the lowering of the excitation energies of the states as well as the increase of the $B(E2)$ values. As to the non-yrast states, the increase of the energies of the 2^+ and 3^+ states with respect to those of the g.s. band is also correctly reproduced. The correspondence between experimental and predicted states is one to one, with just one position inversion of the 2_3^+ and 3_1^+ states in ^{146}Nd (whose experimental energies, however, differ by only 10 keV). A reasonable agreement is obtained for the $E2$ reduced transition strengths, whereas a precise comparison for the $M1$ reduced transition strengths is hampered by the large experimental uncertainties. However, it is to be noted that, in most cases, the non-yrast 2^+ states decay via a transition having a sizable $M1$ component in competition with a pure $E2$ transition and that many transitions deexciting the 3^+ states have $M1$ components. The possibility of reproducing the intensity ratios and the mixing ratios of the transitions is based on a reliable evaluation of the $M1$ transition strength.

In the approach followed in the present work, where both χ_π and χ_ν were kept fixed at $-\sqrt{7}/2$, the change in structure due to the neutron distribution (directly related to the value of χ_ν) is not taken explicitly into account. Therefore, a test was performed on the influence of a change of χ_ν (keeping χ_π fixed to $-\sqrt{7}/2$) on the final results. The calculations were limited to ^{146}Nd, taken as an example because, having a few valence neutrons ($N_\nu = 2$), it is expected to be more sensitive to a variation of χ_ν.

The whole procedure described in Sec. II to determine the Hamiltonian parameters for $\chi_\nu = -\sqrt{7}/2$ was repeated for χ_ν equal to -0.6 and 0. The analysis of the e.m. properties was performed by using for the effective charges and gyromagnetic factors the values reported in Sec. II for ^{146}Nd.

The results of this test, as far as parameters, F spins, and excitation energies are concerned, are shown in Fig. 9. One can notice the limited influence of χ_ν on the Hamiltonian parameters (Fig. 9, left). As to the excitation energies (Fig. 9, middle), important differences are only observed for the values predicted for the 2_2^+ and 3_2^+ states and in this case the best matching to the experimental values is obtained for $\chi_\nu = -\sqrt{7}/2$. The maximum change of α^2 (Fig. 9, right) for increasing χ_ν is also rather limited (less than 15%).

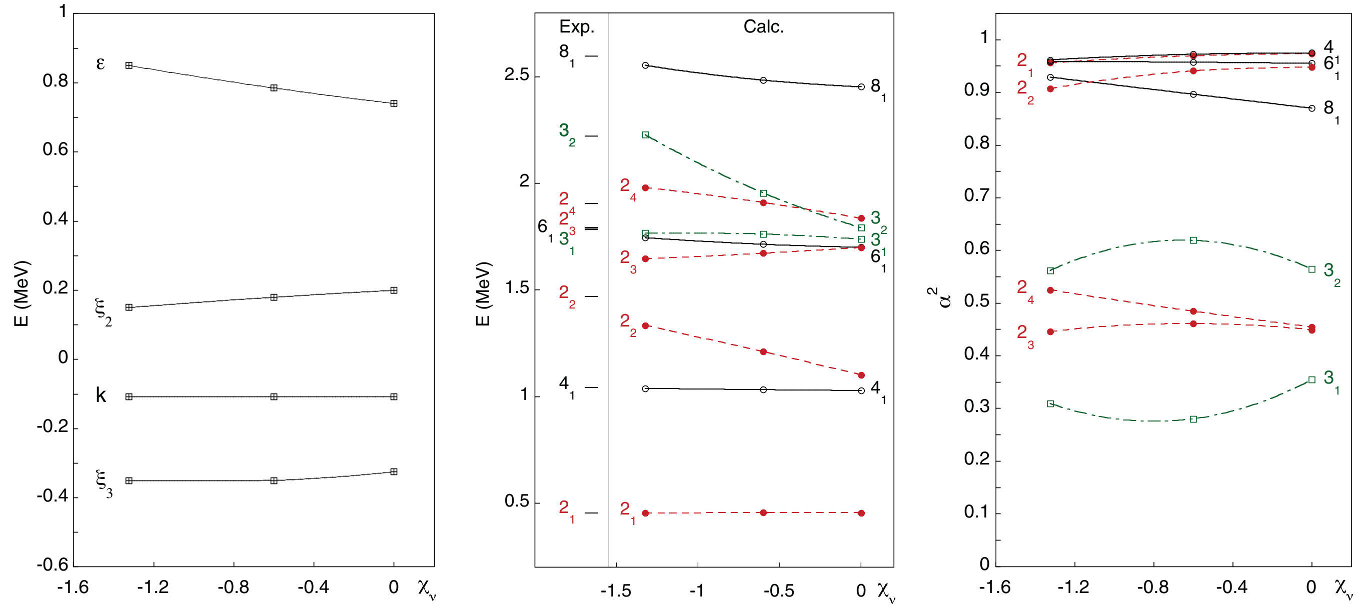

FIG. 9. (Color online) Hamiltonian parameters (left), excitation energies (middle), and squared amplitude of the $F = F_{\max}$ component α^2 (right) of the indicated states in ^{146}Nd, as a function of χ_ν. The Majorana parameter ξ_1 was kept to 1.2 MeV (see text).

The values of $Q(2_1^+)$ and of $B(E2)$ strengths and mixing ratios of the transitions deexciting the relevant states, evaluated for the three values of χ_ν, are reported in Fig. 10, together with the experimental data. The value of χ_ν adopted in the present work seems preferable on the basis of the comparison on $Q(2_1^+)$ and $B(E2; 2_1^+ \rightarrow 0_1^+)$. No additional test, necessary to draw definite conclusions, is however provided by the $B(E2)$ values of the $2_2^+ \rightarrow 0_1^+$, $2_2^+ \rightarrow 2_1^+$, and $4_1^+ \rightarrow 2_1^+$ transitions because of the large or lacking errors of the experimental data.

All three values of χ_ν predict values of the mixing ratios (Fig. 10, right) in agreement with experimental data, apart from $\delta(2_2^+ \rightarrow 2_1^+)$ which, for $\chi_\nu = -0.6$ ($\delta = 95$), is incompatible with the experimental value. Noteworthy, for $\chi_\nu = -1.32$ also the negative sign of $\delta(2_3^+ \rightarrow 2_1^+)$ and $\delta(2_4^+ \rightarrow 2_1^+)$ is reproduced.

From Figs. 9 and 10, one can conclude that for $\chi_\nu = -\sqrt{7}/2$ it is possible to achieve a description of the lighter isotopes at least comparable to that obtained by adopting larger values for this parameter. To summarize, it appears that considering one more parameter (χ_ν) does not lead to any improvement of the predicted quantities when compared to the experimental ones, so it is preferable to keep the parameters of the IBA-2 Hamiltonian to a minimum.

B. ^{150}Nd

In ^{150}Nd, which is the best studied among the heavier isotopes, the parameter P [$P = (N_p N_n)/(N_p + N_n)$] [64] has the value 4.4, which is in the range of values (4–5) characterizing the nuclide representing the element of separation between the transitional region and that of strong deformation. This isotope was the subject of several studies [1,4,65–67] aimed at investigating to what extent it can be considered a good example of an X(5)-like nucleus. Such a topic is not considered here, because the comparison of IBA-2 calculations and X(5) predictions with the experimental data are presented in a separate paper.

The results of the present study are summarized in Fig. 11. Here, in addition to the $B(E2)$ values reported in Ref. [53], are shown the $B(E2)$ values of the $2_2^+ \rightarrow 0_2^+$ transition and of the transitions deexciting the 4_2^+, 4_3^+, and 10_1^+ states, taken from Ref. [4]. The $B(E2; 12_1^+ \rightarrow 10_1^+)$ value was deduced from the lifetime of the 12_1^+ state reported in Ref. [68]. The mixing ratios of the $2_2^+ \rightarrow 2_1^+$ and $4_2^+ \rightarrow 4_1^+$ transitions are from Ref. [69].

By comparing Figs. 6, 7, 8, and 11, a clear change in the structure of ^{150}Nd with respect to the lighter isotopes is apparent. Three bands are present in its excitation energy pattern, i.e., the g.s. band, which shows a quasirotational pattern with large $B(E2)$ values, a well-developed band based on the 0_2^+ state, at an energy close to that of the 6_1^+ state, and a band, based on the 2_3^+ state, at an energy close to that of the 8_1^+ state. The slope of the normalized excitation energies of the non-yrast 2^+ and 3^+ states from ^{148}Nd to ^{150}Nd has a sharp increase with respect to that observed between two neighboring lighter isotopes, as expected for a nucleus approaching the SU(3) region.

Since in ^{152,154,156}Nd the experimental information is actually limited to the g.s. band, it turns out that ^{150}Nd is the only isotope, among those considered, where non-yrast states with $J > 3$ can be taken into account in the analysis for a useful comparison.

The agreement obtained for the excitation energies (apart from that of the 0_2^+ state), $B(E2)$ strengths, intensity ratios, and mixing ratios is rather good. In particular, one can notice that the maximum $B(E2)$ value, observed for the $8_1^+ \rightarrow 6_1^+$ transition, is correctly predicted.

The reasonable description obtained for the complex energy pattern displayed by $^{144-150}$Nd isotopes is related to the

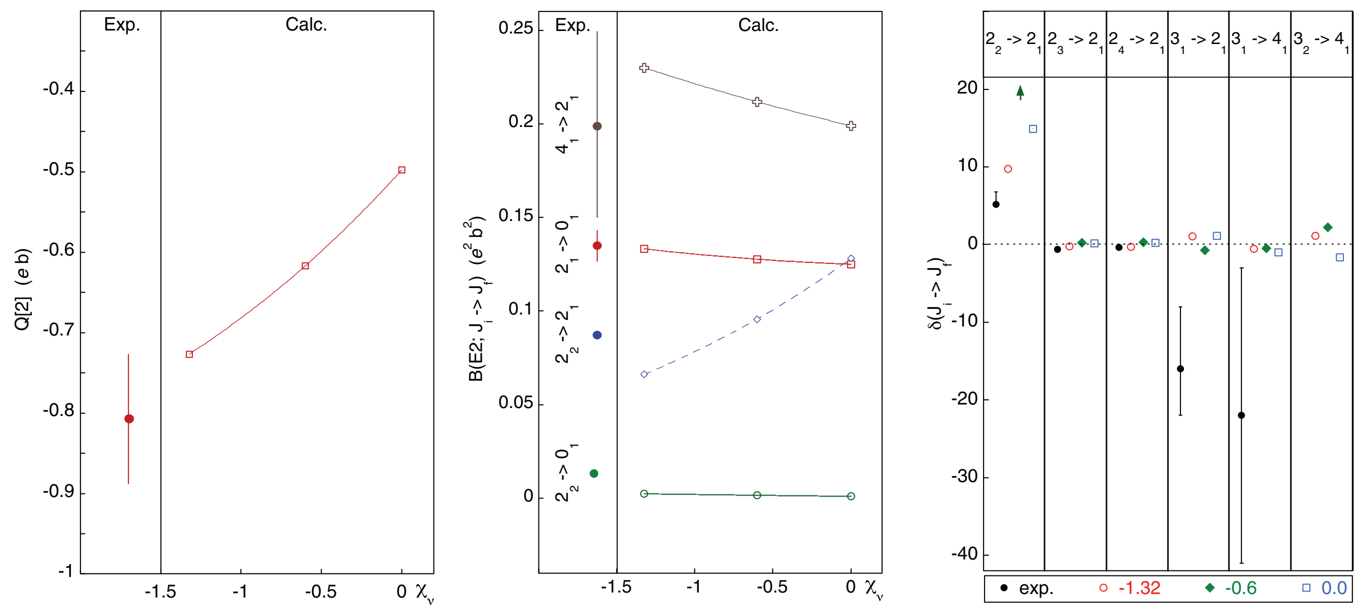

FIG. 10. (Color online) The experimental quadrupole moment of the 2_1^+ state (left), the $B(E2)$ strengths (middle), and the $\delta(E2/M1)$ mixing ratios (right) of the indicated transitions, in ^{146}Nd, are compared to the values calculated for $\chi_\nu = -1.32$ $(-\sqrt{7}/2)$, -0.6, and 0. In the middle panel the experimental values of the $2_2^+ \to 0_1^+$ and $2_2^+ \to 2_1^+$ transitions are reported without errors (see caption of Fig. 7); the calculated values for the $2_2^+ \to 2_1^+$ transition are connected by a dashed line. In the right panel an arrow is reported for $\delta(2_2^+ \to 2_1^+)$ corresponding to $\chi_\nu = -0.6$, because the calculated value (95) lies outside the adopted range for the vertical scale. The error bar(s) for the $2_2^+ \to 2_1^+$, $2_3^+ \to 2_1^+$, and $2_4^+ \to 2_1^+$ transitions are included in the solid circle representing the experimental value.

symmetry character predicted for the states considered. The states belonging to the g.s. band turn out to have FS character. The α^2 value of the 2^+ and 3^+ states is reported in Fig. 12, as a function of A, together with the calculated excitation energies, normalized to that of the 2_1^+ state. It is seen that the 2_2^+ state, as the 2_1^+ state, has quite a pure FS character. In the lighter isotopes the strength of the lowest 2^+ (3^+) MS state is shared by the 2_3^+ and 2_4^+ $(3_1^+$ and $3_2^+)$ states.

As to ^{144}Nd, the identification of the 2_3^+ state as the lowest MS state was proposed a long time ago by Hamilton *et al.* [70] by comparing excitation energy and decay properties of this state with those predicted by the U(5) symmetry. In Ref. [63] the fragmentation of the 2^+ mixed-symmetry mode in this isotope was studied both experimentally and theoretically, in the framework of the IBA-2 model. It was found that the MS strength is predominantly spread over the 2_3^+ and 2_4^+ states with some little strength into the 2_2^+ and 2_5^+ states. The present result is in agreement with such a conclusion.

The abrupt change of the α^2 value for the 2_3^+ and 2_4^+ $(3_1^+$ and $3_2^+)$ states from ^{148}Nd to ^{150}Nd originates from the abrupt increase of deformation. The lowest 2^+ (3^+) MS state moves to high energy so the 2_4^+ (3_2^+) state turns out to have a pure MS character. This is just to be expected for a transition from the U(5) limit (where the lowest MS state is the 2^+ MS state) to the SU(3) limit (where the lowest one is the 1^+ MS state). As to the non-yrast states of $J > 3$ in ^{150}Nd, the calculations predict a sharing of FS and MS components between the 4_3^+ $(\alpha^2 = 0.47)$ and the 4_4^+ $(\alpha^2 = 0.53)$ states, whereas the 4_2^+ $(\alpha^2 = 0.96)$ and 6_2^+ $(\alpha^2 = 0.87)$ states have a predominantly FS character.

C. ^{152,154,156}Nd

The structure of the heavier ^{152,154,156}Nd isotopes is close to that of the SU(3) symmetry, as seen in Fig. 4. The comparison between experimental and calculated data concerning the g.s. bands in ^{152,154,156}Nd is shown in Fig. 13.

The experimental information on transition probabilities is limited to the transitions deexciting the lowest levels in ^{152}Nd, the 2_1^+ states in ^{154}Nd, and the 12^+, 14^+, and 16^+ states in all three isotopes. The $B(E2; 2_1^+ \to 0_1^+)$ value [95(25) W.u.] in ^{154}Nd is hardly compatible with the increasing value observed for this quantity along the isotopic chain, which has already attained the values of 121(9) W.u. in ^{150}Nd and 159(11) W.u. in ^{152}Nd.

The lifetimes of the 12^+, 14^+, and 16^+ states in the three isotopes, measured in the spontaneous fission of a ^{248}Cm source [71], were deduced from the analysis of the Doppler-broadened line shapes during the stopping in the source material of the Nd fragments. Because of the difficulty in the evaluation of the different causes of uncertainties, the errors are not quoted, so the deduced $B(E2)$ values can only be taken as an indication of the fact that no dramatic reduction in their values (which could mean an abrupt change in their structures) shows up for higher spin levels.

Very few spectroscopic data are available for ^{152,154,156}Nd in addition to those concerning the g.s. band. Indeed, only one non-yrast state was definitely identified in the three isotopes, i.e., the 0^+ state at 1.139 MeV in ^{152}Nd. Its energy is close to that predicted for the 0_3^+ state (1.097 MeV), but the deexciting transitions were not observed, which makes difficult its interpretation.

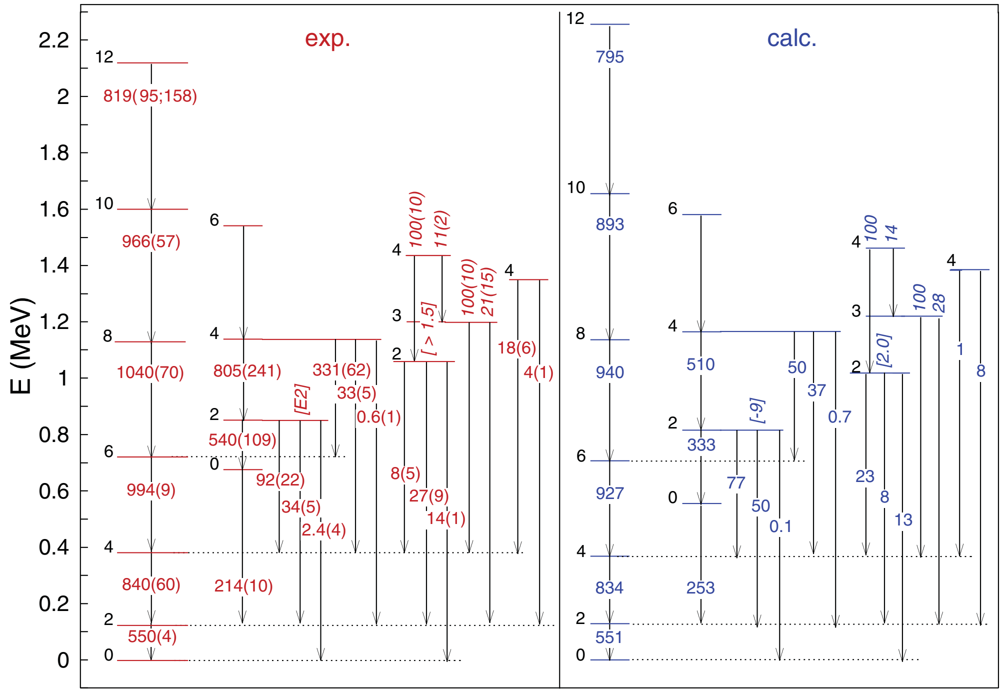

FIG. 11. (Color online) As in Fig. 6, but for ^{150}Nd. The values reported for the $B(E2; 4_2^+ \to 4_1^+)$ and $B(E2; 4_3^+ \to 4_1^+)$ strengths are from Ref. [4]; they were determined by assuming for the transitions a pure $E2$ character. The intensity ratios of the transitions deexciting the 4_2^+ state are unknown. To simplify the figure, the intensity ratios of the transitions deexciting the 2_2^+ and 2_3^+ states are not shown; however, an idea of how closely the calculations reproduce their values can be obtained by comparing the experimental and calculated values of the reported $B(E2)$ and mixing ratios.

The states belonging to the g.s. bands in the three isotopes turn out to have a pure fully symmetric character with an α^2 value close to 1. As seen from Fig. 13, the excitation energies are well reproduced as well as the $B(E2)$ strengths of the transitions connecting the low-lying states in ^{152}Nd. The smooth increase predicted for the $B(E2; 2_1^+ \to 0_1^+)$ value

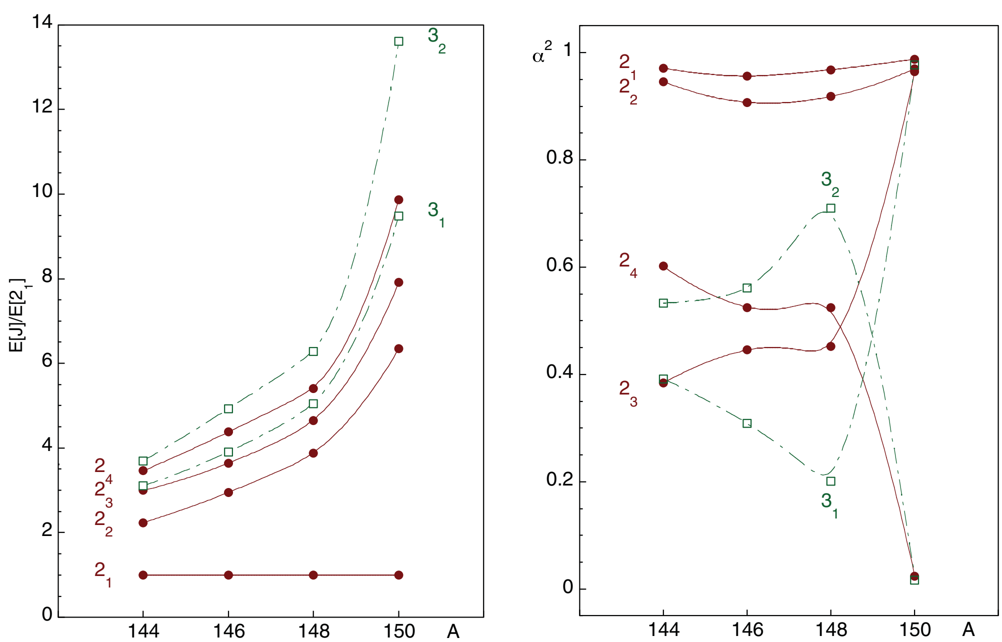

FIG. 12. (Color online) Predicted *normalized* energies (left) and squared amplitudes of the $F = F_{\max}$ component, α^2 (right), of the lowest 2^+ (solid circles) and 3^+ (open squares) states as a function of the mass number A.

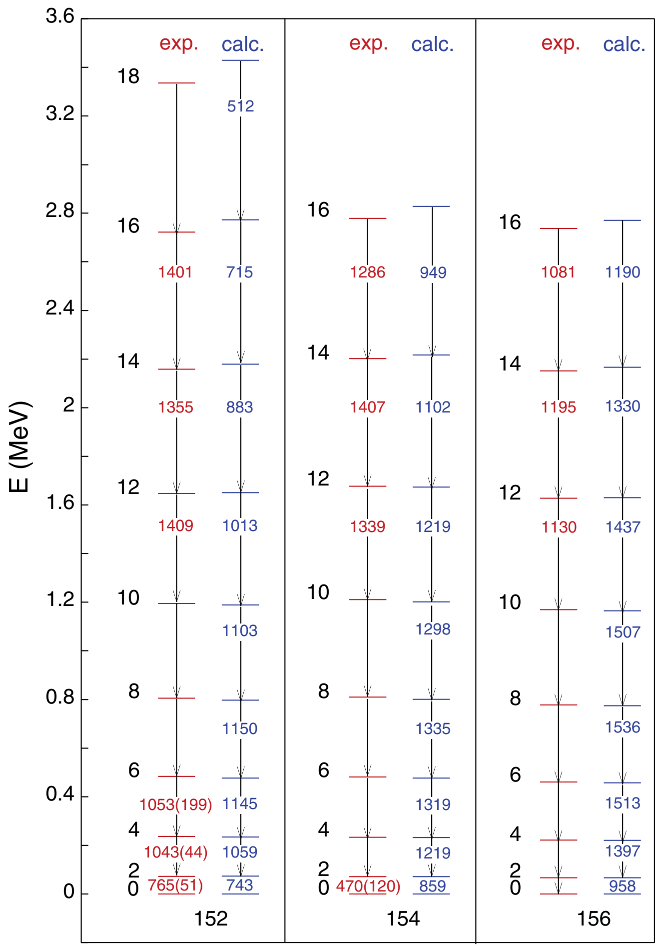

FIG. 13. (Color online) Experimental excitation energies and $B(E2)$ transition strengths are compared to the calculated ones in $^{152-156}$Nd. The $B(E2)$ values are given in 10^{-3} e^2 b^2 units.

in going from ^{152}Nd to ^{156}Nd is not compatible with the experimental value in ^{154}Nd, whose value, however, seems to be questionable.

IV. CONCLUSIONS

The evolution of the nuclear structure, from a spherical to an axially deformed shape, of neodymium isotopes in going from ^{144}Nd to ^{156}Nd was studied in the framework of the IBA-2 model, taking also into account states of possible mixed-symmetry character. A very schematic Hamiltonian, made up by the d-boson energy term, the boson π, ν quadrupole interaction (with $\chi_\pi = \chi_\nu = -\sqrt{7}/2$), and the Majorana operator was used.

States clearly displaying a noncollective structure were excluded from the analysis, and this led to a drastic reduction in the number of levels considered, in particular in $^{144-148}$Nd. The procedure followed to fix the Majorana parameters was illustrated, pointing out the different role played by ξ_1, ξ_2, and ξ_3 in determining the excitation energy patterns. The trend displayed by ξ_2 and ξ_3 at the beginning of the $N = 82$–126 shell turns out to be similar to that found [50,54] at the beginning of the $N = 50$–82 shell.

The dependence of the calculated quantities on χ_ν was studied for ^{146}Nd without observing significant differences with the results obtained fixing χ_ν at $-\sqrt{7}/2$. The limited influence of χ_ν can be traced to the smallness of the κ/ε ratio in the lighter isotopes, which makes predominant, in the Hamiltonian, the $\hat{n}_d$ term with respect to the $\hat{Q}_\pi^{(\chi_\pi)} \cdot \hat{Q}_\nu^{(\chi_\nu)}$ term.

The parameter e_π was allowed to vary from ^{144}Nd to ^{150}Nd to take into account effects due to a possible $Z = 64$ subshell closure, having kept N_π fixed to 5; g_π was assumed to vary proportionally to e_π.

The IBA-2 predictions were compared to the experimental excitation energies, $Q(2_1^+)$ quadrupole moments, $E2$ reduced transition strengths, relative intensities, and mixing ratios of the deexciting transitions. On the average, the excitation energies are matched to better than 0.3%. A reasonable agreement is obtained for the $E2$ transition strengths, whose values are spread over a large range (three orders of magnitude) along the isotopic chain. Sign and order of magnitude of the $E2/M1$ mixing ratios and intensity ratios are correctly reproduced, apart from a few exceptions, which implies that the values predicted for the $M1$ transition strengths are reliable.

It turns out that all along the isotopic chain the levels of the g.s. band examined in the present work have FS character, whereas states of $J^\pi = 2^+$ and 3^+, having large MS components, were identified in $^{144-148}$Nd. The evolution of the nuclear structure in going from the lighter isotopes to ^{150}Nd concerns also the predominant symmetry character of these states. No experimental information is available on $^{152-156}$Nd isotopes, which could extend the search of possible MS states to these isotopes. Altogether, one can conclude that, even though single-particle degrees of freedom can contribute to the structure of the states in the lighter isotopes, the IBA-2 calculations provide a reasonable description of the U(5) $\rightarrow$ SU(3) evolution observed in even $^{144-156}$Nd isotopes.

ACKNOWLEDGMENTS

Many thanks are due to L. Fortunato and P. Sona for very fruitful discussions.

[1] R. F. Casten and N. V. Zamfir, Phys. Rev. Lett. **87**, 052503 (2001).
[2] J. Holden *et al.*, Phys. Rev. C **63**, 024315 (2001).
[3] Ch. Stoyanov, N. Lo Iudice, N. Tsoneva, and M. Grinberg, Phys. At. Nucl. **64**, 1147 (2001).
[4] R. Krücken *et al.*, Phys. Rev. Lett. **88**, 232501 (2002).
[5] A. Frank, C. E. Alonso, and J. M. Arias, Phys. Rev. C **65**, 014301 (2001).
[6] R. M. Clark *et al.*, Phys. Rev. C **68**, 037301 (2003).
[7] J. E. Garcia-Ramos, J. M. Arias, J. Barea, and A. Frank, Phys. Rev. C **68**, 024307 (2003).

[8] J. M. Arias, C. E. Alonso, A. Vitturi, J. E. Garcia-Ramos, J. Dukelsky, and A. Frank, Phys. Rev. C **68**, 041302 (2003).
[9] C. Hutter *et al.*, Phys. Rev. C **67**, 054315 (2003).
[10] D. J. Rowe, Nucl. Phys. A **745**, 47 (2004).
[11] C. Fransen, N. Pietralla, A. Linnemann, V. Werner, and R. Bijker, Phys. Rev. C **69**, 014313 (2004).
[12] D. Tonev *et al.*, Phys. Rev. C **69**, 034334 (2004).
[13] J. M. Arias, J. E. Garcia-Ramos, and J. Dukelsky, Rev. Lett. **93**, 212501 (2004).
[14] M. A. Caprio and F. Iachello, Phys. Rev. Lett. **93**, 242502 (2004).
[15] M. A. Caprio, Phys. Rev. C **69**, 044307 (2004).
[16] E. A. McCutchan *et al.*, Phys. Rev. C **69**, 024308 (2004).
[17] N. Pietralla and O. M. Gorbachenko, Phys. Rev. C **70**, 011304 (2004).
[18] M. A. Caprio and F. Iachello, Ann. Phys. **318**, 454 (2005).
[19] M. A. Caprio, Phys. Rev. C **72**, 054323 (2005).
[20] A. Dewald *et al.*, J. Phys. G **31**, S1427 (2005).
[21] G. Rosensteel and D. J. Rowe, Nucl. Phys. A **759**, 92 (2005).
[22] D. L. Balabanski *et al.*, Int. J. Mod. Phys. E **15**, 1735 (2006).
[23] R. Fossion, D. Bonatsos, and G. A. Lalazissis, Phys. Rev. C **73**, 044310 (2006).
[24] D. Bonatsos *et al.*, Phys. Lett. B **649**, 394 (2007).
[25] L. M. Robledo, R. R. Rodriguez-Guzman, and P. Sarriguren, Phys. Rev. C **78**, 034314 (2008).
[26] A. F. Mertz *et al.*, Phys. Rev. C **77**, 014307 (2008).
[27] Z. P. Li, T. Niksic, D. Vretenar, J. Meng, G. A. Lalazissis, and P. Ring, Phys. Rev. C **79**, 054301 (2009).
[28] N. Lo Iudice, Ch. Stoyanov, and N. Pietralla, Phys. Rev. C **80**, 024311 (2009).
[29] F. Iachello and A. Arima, *The Interacting Boson Model* (Cambridge University Press, Cambridge, UK, 1987), and references therein.
[30] A. Arima, T. Otsuka, F. Iachello, and I. Talmi, Phys. Lett. B **66**, 205 (1977).
[31] T. Otsuka, A. Arima, and F. Iachello, Nucl. Phys. A **309**, 1 (1978).
[32] A. E. L. Dieperink, O. Scholten, and F. Iachello, Phys. Rev. Lett. **44**, 1747 (1980).
[33] F. Iachello, Phys. Rev. Lett. **85**, 3580 (2000).
[34] F. Iachello, Phys. Rev. Lett. **87**, 052502 (2001).
[35] A. Bohr and B. R. Mottelson, *Nuclear Structure* (Benjamin, New York, 1975).
[36] O. Scholten, Ph.D. Thesis, Groningen, 1980 (unpublished).
[37] O. Scholten, K. Heyde, P. Van Isacker, and T. Otsuka, Phys. Rev. C **32**, 1729 (1985).
[38] P. Van Isacker, H. Harter, A. Gelberg, and P. von Brentano, Phys. Rev. C **36**, 441 (1987).
[39] P. O. Lipas, P. von Brentano, and A. Gelberg, Rep. Prog. Phys. **53**, 1353 (1990), and references therein.
[40] N. V. Zamfir, P. von Brentano, R. F. Casten, and J. Jolie, Phys. Rev. C **66**, 021304 (2002).
[41] V. Werner, P. von Brentano, R. F. Casten, and J. Jolie, Phys. Lett. B **527**, 55 (2002).
[42] I. Talmi, *Simple Models of Complex Nuclei* (Harwood Academic Publishers, Switzerland, 1993).
[43] S. T. Ahmad, W. D. Hamilton, P. Van Isacker, S. A. Hamada, and S. J. Robinson, J. Phys. G: Nucl. Part. Phys. **15**, 93 (1989).
[44] T. Otsuka and N. Yoshida, Program NPBOS Japan Atomic Energy Research Institute Report No. JAERI-M85-094, 1985 (unpublished).
[45] D. D. Warner and R. F. Casten, Phys. Rev. C **28**, 1798 (1983).
[46] P. O. Lipas, P. Toivonen, and D. D. Warner, Phys. Lett. B **155**, 295 (1985).
[47] R. F. Casten, D. D. Warner, D. S. Brenner, and R. L. Gill, Phys. Rev. Lett. **47**, 1433 (1981).
[48] A. Wolf and R. F. Casten, Phys. Rev. C **36**, 851 (1987).
[49] I. Talmi, Phys. Lett. B **405**, 1 (1997).
[50] A. Giannatiempo, A. Nannini, and P. Sona, Phys. Rev. C **58**, 3316 (1998).
[51] A. Giannatiempo, A. Nannini, and P. Sona, Phys. Rev. C **58**, 3335 (1998).
[52] J. Margraf *et al.*, Phys. Rev. C **47**, 1474 (1993).
[53] NNDC database, [http://nndc.bnl.gov].
[54] A. Giannatiempo, A. Nannini, P. Sona, and D. Cutoiu, Phys. Rev. C **52**, 2969 (1995).
[55] N. J. Stone, At. Data Nucl. Data Tables **90**, 75 (1975).
[56] C. De Coster and K. Heyde, Int. J. Mod. Phys. A **4**, 3665 (1989).
[57] F. Iachello, Phys. Rev. Lett. **53**, 1427 (1984).
[58] J. Holden *et al.*, Phys. Lett. B **493**, 7 (2000).
[59] C. R. Fitzpatrick *et al.*, Phys. Rev. C **78**, 034309 (2008).
[60] A. M. Demidov, L. I. Govor, V. A. Kurkin, and I. V. Mikhailov, Phys. At. Nucl. **67**, 1884 (2004).
[61] A. Giannatiempo, P. Sona, and A. Nannini, Phys. Rev. C **62**, 044302 (2000).
[62] K. S. Krane and R. M. Steffen, Phys. Rev. C **2**, 724 (1970).
[63] S. F. Hicks, C. M. Davoren, W. M. Faulkner, and J. R. Vanhoy, Phys. Rev. C **57**, 2264 (1998).
[64] R. F. Casten, *Nuclear Structure from a Simple Perspective* (Oxford University Press, New York, 2000).
[65] R. M. Clark *et al.*, Phys. Rev. C **67**, 041302 (2003).
[66] R. F. Casten, N. V. Zamfir, and R. Krücken, Phys. Rev. C **68**, 059801 (2003).
[67] R. V. Jolos and P. von Brentano, Phys. Rev. C **80**, 034308 (2009).
[68] M. Zielinska, Int. J. Mod. Phys. E **13**, 71 (2004).
[69] A. M. Demidov, L. I. Govor, V. A. Kurkin, and I. V. Mikhailov, Phys. At. Nucl. **69**, 1173 (2006).
[70] W. D. Hamilton, A. Irbäck, and J. P. Elliott, Phys. Rev. Lett. **53**, 2469 (1984).
[71] A. G. Smith *et al.*, Phys. Rev. Lett. **73**, 2540 (1994).